*J. Fluid Mech.* (1975), *vol.* 67, *part* 1, *pp.* 177–196
*Printed in Great Britain*



# Entry flow in a curved pipe

By L.-S. YAO AND S. A. BERGER
Mechanical Engineering Department, University of California, Berkeley

(Received 3 April 1974)

A secondary flow is set up when a fluid flows through a stationary curved pipe. The fluid in the middle of the pipe moves outwards and that near the wall inwards. Dean showed that the dynamical similarity of this fully developed flow depends on a non-dimensional parameter $D = 2(a/R)^{\frac{1}{2}}(a\overline{W}/\nu)$, where $\overline{W}$ is the mean velocity along the pipe, $\nu$ is the coefficient of kinematic viscosity and $a$ is the radius of the pipe, which is bent into a coil of radius $R$. Dean's analysis was limited to small values of $D$. Later, Barua developed an asymptotic boundary-layer theory for large values of $D$ and showed for these values of $D$ that the resistance coefficient $\gamma_c$ is much larger than that for the corresponding straight pipe. The present work deals with the flow in a curved pipe as it develops from a uniformly distributed velocity at the entrance to a fully developed profile. Barua's results for the fully developed flow are adopted as downstream conditions in the present work. The ratio of the entry lengths of the curved pipe and the corresponding straight one is shown to be proportional to $D^{-\frac{1}{2}}$ when $D$ is large. Thus, the entry length for a curved pipe is much shorter than that for the corresponding straight pipe.

## 1. Introduction

The developing secondary flow which is induced by the circular motion of the main body of the fluid in a curved pipe may have important implications for blood flow in the human arterial system. For example, it may play a role in the cholesterol deposition on the vascular wall and hence may be involved in the development of arteriosclerosis. Also, information about the pressure drop in the entry region is important in many branches of engineering to determine the pumping power needed to overcome curvature-induced pressure losses. Finally, the enhanced convective heat exchange in the fluid is of considerable importance in designing heat exchangers in nuclear water reactors.

The problem to be considered is steady incompressible developing flow in the entry region of a circular pipe of radius $a$ coiled in a circle of radius $R$. The entrance velocity is assumed to be uniformly distributed with the value $\overline{W}$, an idealized initial condition which models configurations of practical interest. This entrance condition can be produced by connecting the pipe to a large vessel with an abrupt change in cross-sectional area.

We shall briefly review previous work on fully developed flow in curved pipes and entry flow in straight pipes or channels before describing the physical phenomenon of the developing flow in the entry region of a curved pipe.

Extensive interest has been shown in curved-pipe flow, both theoretically and experimentally (e.g. see Eustice 1911; Taylor 1929). Dean (1927, 1928) found that flow in curved pipes depends primarily on a non-dimensional parameter $D = 2\alpha^{\frac{1}{2}}Re$, where $\alpha = a/R$ and $Re = \overline{W}a/\nu$. For small $D$, a uniformly valid asymptotic solution was derived by Dean as a perturbation of the parabolic velocity profile in a straight pipe. This has been extended, numerically, to a moderate value of $D$ by McConalogue & Srivastava (1968). Earlier, Barua (1963) deduced from experimental results (Harwes 1930, unpublished) that for large $D$ viscous forces are important only in a thin boundary layer near the wall, and that the motion outside the boundary layer is mostly confined to planes parallel to the plane of symmetry of the pipe. With these observations and assumptions, Barua was able to obtain an asymptotic boundary-layer solution; the resistance coefficient obtained from this theory agrees with the observations of White & Adler (see Barua 1963). Recently, Greenspan (1973) presented a finite-difference solution covering the whole range of Dean numbers for laminar flow. However, the numerical viscosity inherent in the finite-difference scheme may have overwhelmed the actual viscosity and therefore the results may be invalid for large $D$. Time-dependent fully developed flow in curved pipes was analysed by Lyne (1970) and Zalosh & Nelson (1973).

*Straight pipe*

Previous work on developing flow in straight pipes and channels falls into the following four categories: (i) linearizations of the momentum equations; (ii) two-zone models, in which a boundary-layer flow matches with the downstream perturbation solution for the fully developed flow; (iii) momentum-integral techniques; (iv) finite-difference solutions. Recently, Morihara & Cheng (1973) presented a finite-difference solution of the complete Navier–Stokes equations for entry flow in a two-dimensional channel. They used Stokes flow ($Re = 0$) as the initial solution of the Navier–Stokes equations, then generated the solution for larger Reynolds number by iterating on the quasi-linearized Navier–Stokes equations. A fairly complete list of papers representative of each of the above-mentioned approaches is given by Morihara & Cheng (1973). Time-dependent entry flow in a deformable pipe has been studied by Kuchar & Ostrach (1971). Briley (1972) used an alternating direction implicit method to integrate the momentum equations, without streamwise diffusion terms. However, the validity of a parabolic-flow approximation in the entry region of pipes needs further justification. From a critical analysis of the entry flow problem, Van Dyke (1970) pointed out that there are two characteristic lengths in channel entry flow: $a$, the half-width of the channel, and $aRe$. Most of the early work on this problem is only valid for downstream distances $O(aRe)$. Van Dyke obtained a solution in the upstream region, for distances $O(a)$, and so remedied the discrepancy between the earlier theoretical results and the experimental data near the entrance of the channel. Independently, a similar, more detailed mathematical analysis was given by Wilson (1971).

*Curved pipe*

Now we shall briefly discuss the nature of developing flows in curved pipes. The flow appears to develop as follows (Singh 1974). As the fluid enters the pipe, a boundary layer like that in a straight pipe develops on the wall but with a small azimuthal component of velocity due to the inwardly directed pressure gradient, the latter arising from the circular nature of the main central flow. The displacement effect of the boundary layer in turn causes an acceleration of the flow in the central core plus a secondary flow in the cross-sectional plane. Initially there is an inward flow from the entire pipe circumference, with two singularities in the central region, a node-like sink at the origin and a saddle-point-like stagnation point; the latter singularity moves outwards as the fluid moves downstream, finally vanishing as the cross-flow (from the inside to the outside of the bend) sets in. (For further details, plus the interesting consequences this flow picture has on the location of the point of maximum shear, see Singh (1974).) The flow development just described all occurs within a distance $O(a)$ from the entrance. The matched asymptotic solution for this region (Singh 1974) breaks down at a distance $O((aR)^{\frac{1}{2}})$, corresponding, physically, to the point beyond which the effect of the centrifugal force, initially small, becomes as important as inertia and viscous forces within the boundary layer. The matched asymptotic solution developed in turn for this region apparently breaks down at a downstream distance $O(aRe)$. Presumably this last flow region, at distances $O(aRe)$, is the region of transition to the fully developed flow (Singh, private communication). Particularly noteworthy in this analysis is that the entry length is of the same order, $aRe$, as for a straight pipe, so that the additional mixing due to the secondary cross-flow appears to have little effect on this important quantity. It might also be noted that for $D \lesssim 1$, since

$$(aR)^{\frac{1}{2}} = (aRe)\,D^{-1},$$

the region up to distances $O((aR)^{\frac{1}{2}})$ is either larger than that up to distances $O(aRe)$ or coincident with it, so that for this case the flow becomes fully developed before centrifugal forces lose their secondary role.

In the high Dean number case, the situation is somewhat different. Centrifugal effects are as important as viscosity and inertia almost from the beginning.† Much of the flow development occurs within a distance $O((aR)^{\frac{1}{2}})$, where these three forces balance. In other words, the motion of the central core of the fluid is quite different for the cases of large and small $D$, and so is the development of the boundary layer. The curvature ratio $\alpha$ is smaller than one for most curved tubes of interest. This means that the variation of the centrifugal force and the pressure gradient directed away from the centre of curvature on a cross-section of the tube is small near the entrance for a uniformly distributed inlet velocity profile. The resultant of the nearly uniformly distributed pressure gradient and the strong centrifugal force will accelerate the fluid in the central core. The flow

† Singh's solution up to distances $O(a)$, in which centrifugal forces are a second-order effect, is, however, uniformly valid for all values of the Dean number. (The authors are indebted to a reviewer for pointing this out.)

is nearly uniform from the inner to the outer wall of the tube (away from the centre of curvature). The boundary layer acts as a reservoir, receiving the fluid moving towards the outer wall, and also as a source of fluid leaving it at the inner wall. This is consistent with mass conservation for the boundary layers in the cross-section of the tube. The resulting cross-flow forms a stagnation-like flow locally along the outer wall of the tube. The convective effect of this locally stagnant flow prevents the secondary boundary layer from growing. Thus, the secondary boundary layer will remain thin as the flow asymptotically approaches the fully developed state (Barua's flow). As will be shown later, the distance at which the fully developed state is reached is $O((aRD)^{\frac{1}{2}})$, or equivalently $O(a\,Re\,D^{-\frac{1}{2}})$, i.e. smaller by a factor $D^{-\frac{1}{2}}$ than the entry length for the case of low or moderate Dean number. The remainder of the paper will be concerned with the entry flow for large $D$.

## 2. Equations of motion

Two different sets of co-ordinates are used in the analysis. (See figure 1.) The toroidal co-ordinates $(r, \psi, \theta)$ are used to describe the motion of fluid close to the pipe wall, where $r$ denotes the distance from the centre of the cross-section of the pipe, $\psi$ the angle between the radius vector and the normal to the plane of symmetry, and $\theta$ the angular distance of the cross-section from the entry of the pipe. Let $(u, v, w)$ denote the corresponding velocity components. The equations of motion are the continuity equation

$$\frac{1}{r}\frac{\partial(ru)}{\partial r}+\frac{u\sin\psi}{R+r\sin\psi}+\frac{1}{r}\frac{\partial v}{\partial\psi}+\frac{v\cos\psi}{R+r\sin\psi}+\frac{1}{R+r\sin\psi}\frac{\partial w}{\partial\theta}=0 \tag{1a}$$

and the Navier–Stokes equations

$$\begin{aligned}
&u\frac{\partial u}{\partial r}+\frac{v}{r}\frac{\partial u}{\partial\psi}+\frac{w}{R+r\sin\psi}\frac{\partial u}{\partial\theta}-\frac{v^2}{r}-\frac{w^2\sin\psi}{R+r\sin\psi}\\
&\quad=-\frac{1}{\rho}\frac{\partial p}{\partial r}+\nu\Bigg\{-\left(\frac{1}{r}\frac{\partial}{\partial\psi}+\frac{\cos\psi}{R+r\sin\psi}\right)\left(\frac{\partial v}{\partial r}+\frac{v}{r}-\frac{1}{r}\frac{\partial u}{\partial\psi}\right)\\
&\qquad+\frac{1}{(R+r\sin\psi)^2}\frac{\partial}{\partial\theta}\left[\frac{\partial u}{\partial\theta}-w\sin\psi+(R+r\sin\psi)\frac{\partial w}{\partial r}\right]\Bigg\},
\end{aligned} \tag{1b}$$

$$\begin{aligned}
&u\frac{\partial v}{\partial r}+\frac{v}{r}\frac{\partial v}{\partial\psi}+\frac{w}{R+r\sin\psi}\frac{\partial v}{\partial\theta}+\frac{uv}{r}-\frac{w^2\cos\psi}{R+r\sin\psi}\\
&\quad=-\frac{1}{\rho r}\frac{\partial p}{\partial\psi}+\nu\Bigg\{\left(\frac{\partial}{\partial r}+\frac{\sin\psi}{R+r\sin\psi}\right)\left(\frac{\partial v}{\partial r}+\frac{v}{r}-\frac{1}{r}\frac{\partial u}{\partial\psi}\right)\\
&\qquad-\frac{1}{(R+r\sin\psi)^2}\frac{\partial}{\partial\theta}\left[w\cos\psi-\frac{\partial v}{\partial\theta}+\frac{R+r\sin\psi}{r}\frac{\partial w}{\partial\psi}\right]\Bigg\},
\end{aligned} \tag{1c}$$

$$\begin{aligned}
&u\frac{\partial w}{\partial r}+\frac{v}{r}\frac{\partial w}{\partial\psi}+\frac{w}{R+r\sin\psi}\frac{\partial w}{\partial\theta}+\frac{w(u\sin\psi+v\cos\psi)}{R+r\sin\psi}\\
&\quad=-\frac{1}{\rho(R+r\sin\psi)}\frac{\partial p}{\partial\theta}+\nu\Bigg\{\left(\frac{\partial}{\partial r}+\frac{1}{r}\right)\left[\frac{\partial w}{\partial r}-\frac{1}{R+r\sin\psi}\left(\frac{\partial u}{\partial\theta}-w\sin\psi\right)\right]\\
&\qquad+\frac{1}{r}\frac{\partial}{\partial\psi}\left[\frac{1}{r}\frac{\partial w}{\partial\psi}-\frac{1}{R+r\sin\psi}\left(\frac{\partial v}{\partial\theta}-w\cos\psi\right)\right]\Bigg\}.
\end{aligned} \tag{1d}$$

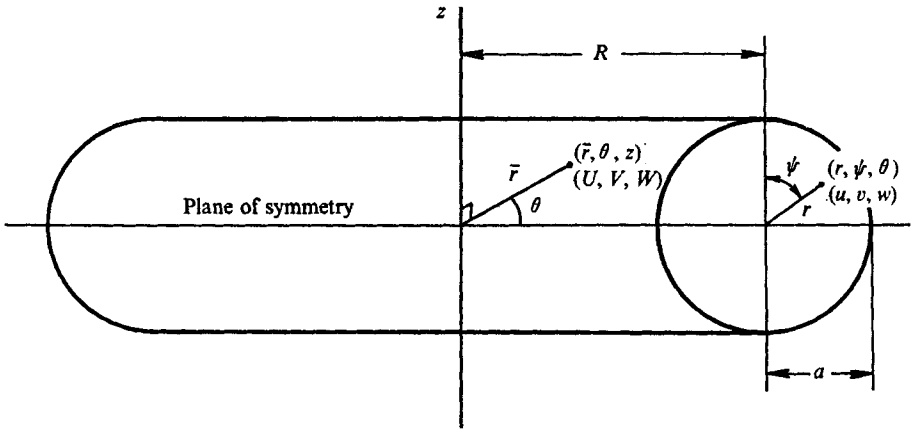


FIGURE 1. Co-ordinate systems.

Cylindrical polar co-ordinates $(\bar{r}, \theta, z)$, with origin at the centre of curvature, are used to describe the motion of fluid far from the pipe wall, with the $z$ axis passing through the centre of curvature and perpendicular to the plane of symmetry of the pipe. Here $(U, V, W)$ will denote the corresponding velocity components. In terms of these co-ordinates, equations (1) are

$$\frac{1}{\bar{r}}\frac{\partial(\bar{r}U)}{\partial\bar{r}}+\frac{\partial V}{\partial z}+\frac{1}{\bar{r}}\frac{\partial W}{\partial\theta}=0, \tag{2a}$$

$$U\frac{\partial U}{\partial\bar{r}}+V\frac{\partial U}{\partial z}+\frac{W}{\bar{r}}\frac{\partial U}{\partial\theta}-\frac{W^2}{\bar{r}} = -\frac{1}{\rho}\frac{\partial P}{\partial\bar{r}}+\nu\left\{\frac{\partial^2 U}{\partial\bar{r}^2}+\frac{1}{\bar{r}}\frac{\partial U}{\partial\bar{r}}+\frac{1}{\bar{r}^2}\frac{\partial^2 U}{\partial\theta^2}+\frac{\partial^2 U}{\partial z^2}-\frac{U}{\bar{r}^2}-\frac{2}{\bar{r}^2}\frac{\partial W}{\partial\theta}\right\}, \tag{2b}$$

$$U\frac{\partial V}{\partial\bar{r}}+V\frac{\partial V}{\partial z}+\frac{W}{\bar{r}}\frac{\partial V}{\partial\theta} = -\frac{1}{\rho}\frac{\partial P}{\partial z}+\nu\left[\frac{\partial^2 V}{\partial\bar{r}^2}+\frac{1}{\bar{r}}\frac{\partial V}{\partial\bar{r}}+\frac{1}{\bar{r}^2}\frac{\partial^2 V}{\partial\theta^2}+\frac{\partial^2 V}{\partial z^2}\right], \tag{2c}$$

$$U\frac{\partial W}{\partial\bar{r}}+V\frac{\partial W}{\partial z}+\frac{W}{\bar{r}}\frac{\partial W}{\partial\theta}+\frac{UW}{\bar{r}} = -\frac{1}{\rho\bar{r}}\frac{\partial P}{\partial\theta}+\nu\left[\frac{\partial^2 W}{\partial\bar{r}^2}+\frac{1}{\bar{r}}\frac{\partial W}{\partial\bar{r}}+\frac{1}{\bar{r}^2}\frac{\partial^2 W}{\partial\theta^2}+\frac{\partial^2 W}{\partial z^2}+\frac{2}{\bar{r}^2}\frac{\partial W}{\partial\theta}-\frac{W}{\bar{r}^2}\right]. \tag{2d}$$

## 3. Motion outside the boundary layer

Owing to the cross-flow, developing flow in a curved pipe requires a much shorter entrance length to become fully developed than the corresponding flow in a straight pipe. The characteristic length of the developing flow in a curved pipe can be shown, from the principles of conservation of mass and momentum, to be $O((aR)^{\frac{1}{2}})$ (Yao 1973), which is different from the characteristic lengths $O(a)$ and $O(aRe)$ for a straight pipe.

We now can introduce the following non-dimensional variables (outer variables):

$$r_0=(\bar{r}-R)/a,\quad z_0=z/a,\quad \theta_0=R\theta/(Ra)^{\frac{1}{2}},$$
$$u_0=U/\alpha^{\frac{1}{2}}\overline{W},\quad w_0=W/\overline{W},\quad v_0=V/\alpha^{\frac{1}{2}}\overline{W},$$
$$P_0=P/\rho\overline{W}^2.$$

Equations (2) become

$$\frac{1}{1+\alpha r_0}\frac{\partial[(1+\alpha r_0)u_0]}{\partial r_0}+\frac{\partial v_0}{\partial z_0}+\frac{1}{1+\alpha r_0}\frac{\partial w_0}{\partial \theta_0}=0, \tag{3a}$$

$$u_0\frac{\partial u_0}{\partial r_0}+v_0\frac{\partial u_0}{\partial z_0}+\frac{w_0}{1+\alpha r_0}\frac{\partial u_0}{\partial \theta_0}-\frac{w_0^2}{1+\alpha r_0}=-\frac{1}{\alpha}\frac{\partial P_0}{\partial r_0}+O(D^{-1}), \tag{3b}$$

$$u_0\frac{\partial v_0}{\partial r_0}+v_0\frac{\partial v_0}{\partial z_0}+\frac{w_0}{1+\alpha r_0}\frac{\partial v_0}{\partial \theta_0}=-\frac{1}{\alpha}\frac{\partial P_0}{\partial z_0}+O(D^{-1}), \tag{3c}$$

$$u_0\frac{\partial w_0}{\partial r_0}+v_0\frac{\partial w_0}{\partial z_0}+\frac{w_0}{1+\alpha r_0}\frac{\partial w_0}{\partial \theta_0}+\frac{\alpha u_0 w_0}{1+\alpha r_0}=-\frac{1}{1+\alpha r_0}\frac{\partial P_0}{\partial \theta_0}+O(D^{-1}). \tag{3d}$$

In the limit $D\to\infty$, the above set of equations represents the first-order inviscid flow. It is a set of three-dimensional, nonlinear, elliptic partial differential equations. The boundary conditions are as follows.

(i) Uniform entrance flow:

$$w_0=1, \quad u_0=v_0=0 \quad \text{at} \quad \theta_0=0 \quad \text{for} \quad r_0^2+z_0^2\leqslant 1. \tag{4a}$$

(ii) Slip boundary condition:

$$u_0\sin\psi+v_0\cos\psi=0 \quad \text{at} \quad r_0^2+z_0^2=1, \quad \psi=\tan^{-1}(z_0/r_0). \tag{4b}$$

(iii) Matching condition:

$$(w_0,u_0,v_0)\to\text{fully developed flow as} \quad \theta_0\to\infty \quad \text{for} \quad r_0^2+z_0^2\leqslant 1. \tag{4c}$$

From (3) we see that the centrifugal force is of the same order of magnitude as the other inertial forces. Also, the pressure gradients in the cross-sectional plane are of order $\alpha$, compared with the pressure gradient along the axis of the pipe.

Equations (3) with conditions (4) constitute a well-posed boundary-value problem. An analytical solution is unlikely to be found owing to the highly nonlinear inertia terms; at the same time a full numerical solution offers formidable problems owing to the complicated three-dimensional nature of the equations. Thus, we shall adopt the simplifications mentioned in the introduction, namely, that the central cross-flow is essentially parallel to the plane of symmetry. This appears to be nearly the case for the fully developed flow (Barua 1963) and should therefore be appropriate as the flow approaches this state. This assumption simplifies (3) by neglecting motion in the $z_0$ direction. The resulting equations show that the geometric influence is small for $\alpha<1$. The reduced equations are

$$\partial[(1+\alpha r_0)u_0]/\partial r_0+\partial w_0/\partial\theta_0=0, \tag{5a}$$

$$u_0\frac{\partial u_0}{\partial r_0}+\frac{w_0}{1+\alpha r_0}\frac{\partial u_0}{\partial \theta_0}-\frac{w_0^2}{1+\alpha r_0}=-\frac{1}{\alpha}\frac{\partial P_0}{\partial r_0}, \tag{5b}$$

$$u_0\frac{\partial w_0}{\partial r_0}+\frac{w_0}{1+\alpha r_0}\frac{\partial w_0}{\partial \theta_0}+\frac{\alpha u_0 w_0}{1+\alpha r_0}=-\frac{1}{1+\alpha r_0}\frac{\partial P_0}{\partial \theta_0}. \tag{5c}$$

If terms of order $\alpha$ and smaller are neglected, apart from the centrifugal force term, equations (5) are the inviscid equations of motion describing fluid motion in a straight cylinder with the primary flow along the axis of the cylinder. The existence of the centrifugal force presents the major mathematical difficulty in solving the above equations. But the solution for the fully developed flow in a curved pipe for large Dean number (Barua 1963) shows that the dominant part of the axial velocity component $w_0$ can be fairly well approximated by an almost linear function in $r_0$ with positive slope. Thus we can study, approximately, the development of the axial velocity in the $\theta$ direction by writing it in the form

$$w_0 = f_1(\theta_0) - f_2(\theta_0)/(1+\alpha r_0), \tag{6}$$

where $f_1$ and $f_2$ are unknown functions. We note that

(i) $f_1 - f_2$ represents the average main axial flow, which is accelerated owing to the displacement of the boundary layer developing along the wall of the pipe;

(ii) $\alpha f_2$ indicates the way the axial velocity adjusts, owing to the curvature of the pipe, to balance the effect of the centrifugal force.

From (5*a*) and (6) the velocity component $u_0$ can be written as

$$u_0 = \frac{f_3(\theta_0)}{1+\alpha r_0} - \frac{f_1'(\theta_0)\, r_0}{1+\alpha r_0} + \frac{f_2'(\theta_0)\, r_0}{(1+\alpha r_0)^2} \tag{7}$$

for small $\alpha$, where $f_3$ is another unknown function.

## 4. Flow in the boundary layer

Equations (1) are normalized by introducing non-dimensional variables (inner variables) reflecting the fact that viscous forces are important near the pipe wall:

$$r_1 = (a-r)/a(2/D)^{\frac{1}{2}}, \quad \theta_1 = \theta_0,$$

$$u_1 = -u/(2\alpha/D)^{\frac{1}{2}}\,\overline{W}, \quad v_1 = v/\alpha^{\frac{1}{2}}\overline{W}, \quad w_1 = w/\overline{W},$$

$$p_1 = p/\rho\,\overline{W}^2.$$

The equations become

$$\frac{\partial u_1}{\partial r_1} + \frac{\partial v_1}{\partial \psi} + \frac{\alpha v_1 \cos\psi}{1+\alpha\sin\psi} + \frac{1}{1+\alpha\sin\psi}\frac{\partial w_1}{\partial \theta_1} = 0,$$

$$\partial p_1/\partial r_1 = 0,$$

$$u_1\frac{\partial v_1}{\partial r_1} + v_1\frac{\partial v_1}{\partial \psi} + \frac{w_1}{1+\alpha\sin\psi}\frac{\partial v_1}{\partial \theta_1} - \frac{w_1^2\cos\psi}{1+\alpha\sin\psi} = -\frac{1}{\alpha}\frac{\partial p_1}{\partial \psi} + \frac{\partial^2 v_1}{\partial r_1^2},$$

$$u_1\frac{\partial w_1}{\partial r_1} + v_1\frac{\partial w_1}{\partial \psi} + \frac{w_1}{1+\alpha\sin\psi}\frac{\partial w_1}{\partial \theta_1} + \frac{\alpha w_1 v_1\cos\psi}{1+\alpha\sin\psi} = -\frac{1}{1+\alpha\sin\psi}\frac{\partial p_1}{\partial \theta_1} + \frac{\partial^2 w_1}{\partial r_1^2},$$

neglecting terms of order $D^{-\frac{1}{2}}$ and smaller.

These non-dimensional equations are of boundary-layer type, showing no variation in pressure across the thin boundary layer, whose thickness is of order $D^{-\frac{1}{2}}$. The pressure gradients parallel to the pipe wall can be evaluated from the outer solution at the edge of the boundary layer. Since the cross-flow is small

compared with the flow along the axis of the pipe, we can approximate these pressure gradients as

$$-\frac{1}{\alpha}\frac{\partial p_1}{\partial \psi} = -\frac{\overline{w}_0^2 \cos\psi}{1+\alpha\sin\psi},$$

$$-\frac{1}{1+\alpha\sin\psi}\frac{\partial p_1}{\partial \theta_1} = \frac{\overline{w}_0}{1+\alpha\sin\psi}\frac{\partial \overline{w}_0}{\partial \theta_0},$$

where $\overline{w}_0$ is the axial velocity component at the edge of the boundary layer. Substitution of the above into the boundary-layer equations gives

$$\frac{\partial u_1}{\partial r_1}+\frac{\partial v_1}{\partial \psi}+\frac{\alpha v_1\cos\psi}{1+\alpha\sin\psi}+\frac{1}{1+\alpha\sin\psi}\frac{\partial w_1}{\partial \theta_1}=0, \tag{8a}$$

$$u_1\frac{\partial v_1}{\partial r_1}+v_1\frac{\partial v_1}{\partial \psi}+\frac{w_1}{1+\alpha\sin\psi}\frac{\partial v_1}{\partial \theta_1}+\frac{(\overline{w}_0^2-w_1^2)\cos\psi}{1+\alpha\sin\psi}=\frac{\partial^2 v_1}{\partial r_1^2}, \tag{8b}$$

$$u_1\frac{\partial w_1}{\partial r_1}+v_1\frac{\partial w_1}{\partial \psi}+\frac{w_1}{1+\alpha\sin\psi}\frac{\partial w_1}{\partial \theta_1}-\frac{\overline{w}_0}{1+\alpha\sin\psi}\frac{\partial \overline{w}_0}{\partial \theta_0}+\frac{\alpha w_1 v_1\cos\psi}{1+\alpha\sin\psi}=\frac{\partial^2 w_1}{\partial r_1^2}. \tag{8c}$$

A Kármán–Pohlhausen type of approximation is used to solve (8). This consists of assuming an arbitrary form for the velocity distribution in the boundary layer and then requiring that it satisfy the no-slip boundary conditions at the pipe wall, match with the outer solution at the edge of the boundary layer and satisfy the momentum integrals for the boundary layer.

To obtain these integrals, we integrate (8*b*) and (8*c*) across the boundary layer, assumed to be of thickness $\delta_1$:

$$\int_0^{\delta_1}\left(u_1\frac{\partial v_1}{\partial r_1}+v_1\frac{\partial v_1}{\partial \psi}+\frac{w_1}{1+\alpha\sin\psi}\frac{\partial v_1}{\partial \theta_1}\right)dr_1+\int_0^{\delta_1}\frac{(\overline{w}_0^2-w_1^2)\cos\psi}{1+\alpha\sin\psi}\,dr_1=-\left.\frac{\partial v_1}{\partial r_1}\right|_{r_1=0}, \tag{9a}$$

$$\int_0^{\delta_1}\left(u_1\frac{\partial w_1}{\partial r_1}+v_1\frac{\partial w_1}{\partial \psi}+\frac{w_1}{1+\alpha\sin\psi}\frac{\partial w_1}{\partial \theta_1}\right)dr_1$$

$$-\int_0^{\delta_1}\frac{\overline{w}_0}{1+\alpha\sin\psi}\frac{\partial \overline{w}_0}{\partial \theta_0}\,dr_1+\int_0^{\delta_1}\frac{\alpha w_1 v_1}{1+\alpha\sin\psi}\,dr_1=-\left.\frac{\partial w_1}{\partial r_1}\right|_{r_1=0}. \tag{9b}$$

For a thin boundary layer, $u_1$ at $r_1=\delta_1$ is small compared with the other velocity components. Also, $v_1$ at $r_1=\delta_1$ is small for small cross-flow outside the boundary layer. Again, $u_1$, $v_1$ and $w_1$ vanish at $r_1=0$. Hence we have

$$u_1 v_1\big|_0^{\delta_1}=0,$$

$$u_1 w_1\big|_0^{\delta_1}=u_1 w_1\big|_{r_1=\delta_1}\simeq -\overline{w}_0 u_1\big|_{r_1=\delta_1}.$$

We now assume a form for the distribution of velocity through the boundary layer. Simple series expressions which satisfy the required boundary conditions, namely $v_1=w_1=0$ at $r_1=0$, and $v_1=0$, $w_1=\overline{w}_0$ and $\partial v_1/\partial r_1=\partial w_1/\partial r_1=0$ at $r_1=\delta_1$, are

$$\left.\begin{aligned} v_1&=\bar{v}_1(\eta-2\eta^2+\eta^3)=\bar{v}_1\phi_1(\eta),\\ w_1&=\overline{w}_0(2\eta-\eta^2)=\overline{w}_0\phi_2(\eta),\end{aligned}\right\} \tag{10}$$

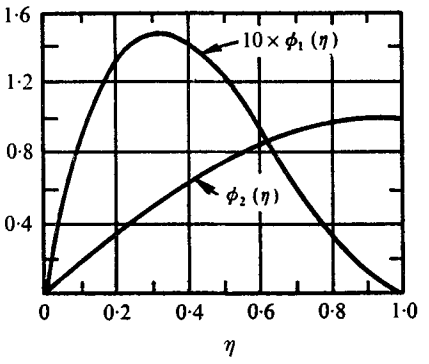


FIGURE 2. Velocity distribution in the boundary layer.

where $\eta = r_1/\delta_1$, and $\bar{v}_1$ and $\bar{w}_0$ are functions of $\psi$ and $\theta_1$. It may be noted that $v_1$ is small and not exactly equal to zero at the edge of the boundary layer; this approximation is, however, not expected to alter the results appreciably. The functions $\phi_1$ and $\phi_2$ are plotted in figure 2. With these particular forms for $\phi_1$ and $\phi_2$, we have

$$\int_0^1 \phi_1 d\eta = \tfrac{1}{12}, \quad \int_0^1 \phi_2 d\eta = \tfrac{2}{3}, \quad \left.\frac{\partial\phi_1}{\partial\eta}\right|_{\eta=0} = 1,$$

$$\int_0^1 \phi_1^2 d\eta = \tfrac{1}{105}, \quad \int_0^1 \phi_2^2 d\eta = \tfrac{8}{15}, \quad \left.\frac{\partial\phi_2}{\partial\eta}\right|_{\eta=0} = 2,$$

$$\int_0^1 \phi_1\phi_2 d\eta = \tfrac{1}{20}.$$

Equations (9) then reduce to

$$\frac{1}{105}\frac{\partial(\delta_1\bar{v}_1^2)}{\partial\psi} + \frac{\alpha}{105}\frac{\delta_1\bar{v}_1^2}{1+\alpha\sin\psi} + \frac{1}{20(1+\alpha\sin\psi)}\frac{\partial}{\partial\theta_1}(\delta_1\bar{w}_0\bar{v}_1) + \frac{7}{15}\frac{\delta_1\bar{w}_0^2\cos\psi}{1+\alpha\sin\psi} = -\frac{\bar{v}_1}{\delta_1}, \tag{11}$$

$$\frac{1}{20}\frac{\partial(\delta_1\bar{w}_0\bar{v}_1)}{\partial\psi} + \frac{\alpha\delta_1\bar{w}_0\bar{v}_1}{20(1+\alpha\sin\psi)} - \frac{7}{15(1+\alpha\sin\psi)}\frac{\partial}{\partial\theta_1}(\delta_1\bar{w}_0^2) - \frac{\bar{w}_0}{12}\frac{\partial}{\partial\psi}(\delta_1\bar{v}_1) + \frac{1}{3(1+\alpha\sin\psi)}\frac{\partial(\delta_1\bar{w}_0^2)}{\partial\theta_1} = -2\frac{\bar{w}_0}{\delta_1}. \tag{12}$$

The unknown quantities $\bar{v}_1$ and $\delta_1$ are to be determined from (11) and (12). The difficulty in solving these equations is the presence of the unknown functions $f_1$ and $f_2$ implicitly in the function $\bar{w}_0$. Rearranging (11) gives

$$\bar{v}_1 = \frac{\delta_1\bar{v}_1}{60}\left[\frac{\partial(\delta_1\bar{v}_1)}{\partial\psi} + \frac{\alpha\delta_1\bar{v}_1}{1+\alpha\sin\psi}\right] - \frac{(\delta_1\bar{v}_1)^2}{40\,\bar{w}_0}\frac{\partial\bar{w}_0}{\partial\psi} + \frac{\delta_1\bar{v}_1}{15(1+\alpha\sin\psi)}\left[\bar{w}_0\frac{\partial\delta_1}{\partial\theta_1} + 2\delta_1\frac{\partial\bar{w}_0}{\partial\theta_1}\right]. \tag{13}$$

This shows that once the product $\delta_1\bar{v}_1$, the mass flow rate of the secondary flow inside the boundary layer, is known, the first three terms on the right-hand side of

(13) can be evaluated. From the solution for fully developed flow in a curved pipe we know that the thickness of the boundary layer varies little with $\psi$, except at the separation point near the rear stagnation point ($\psi = -90°$). Assuming that this is approximately true also for the developing flow, we can evaluate the last two terms on the right-hand side of (13) by approximating $\delta_1$ and $\partial\delta_1/\partial\theta_1$ for different $\theta_1$ by the mean values $\bar{\delta}_1$ and $d\bar{\delta}_1/d\theta_1$ on each cross-section of the tube. The two integral forms of mass conservation derived in the following subsections supply a means of evaluating $\bar{\delta}_1$ and $d\bar{\delta}_1/d\theta_1$ in terms of the inviscid outer solution.

*Conservation of mass along the tube*

Here we consider the relationship between the thickness of the boundary layer and the accelerating inviscid flow. The integral form of mass conservation relating them can be written as

$$\int_{\frac{1}{2}\pi}^{-\frac{1}{2}\pi}\int_0^a \overline{W}r\,dr\,d\psi = \int_{\frac{1}{2}\pi}^{-\frac{1}{2}\pi}\left[\int_0^a W\bar{r}\,d\bar{r} - \int_{a-\delta}^a (W-\overline{W}\bar{w}_0\phi_2)\,a\,dr\right]d\psi,$$

where the term on the left is the amount of fluid that enters the pipe, the first term on the right is the volume flow rate of the accelerating inviscid flow and the second term is the fluid deficit due to the existence of the secondary boundary layer. Using (5), (6) and (10) to carry out the above integrations, and assuming that $\delta_1$ can be approximated by $\bar{\delta}_1(\theta)$, we obtain

$$\bar{\delta}_1 = 1{\cdot}5\,(f_1 - f_2 - 1)/(f_1 - f_2),$$

so that

$$d\bar{\delta}_1/d\theta_1 = 1{\cdot}5\,(f_1-f_2)'/(f_1-f_2)^2, \tag{14}$$

where $\delta_0 = \delta_1(2/D)^{\frac{1}{2}} = \delta/a$, similarly for its mean value.

*Conservation of mass of the secondary flow*

Since there is a cross-flow outside the boundary layer transporting fluid from the inside tube wall $\psi \approx -90°$ to the outside tube wall $\psi \approx 90°$, the boundary layer acts as a reservoir, receiving fluid between approximately $\psi = 0$ and $\psi = 90°$ and releasing it between $\psi = 0$ and $\psi = -90°$. The flow pattern is symmetric with respect to the line $\psi = \pm 90°$. The integral form of this mass conservation is

$$\int_{\psi}^{\frac{1}{2}\pi} Ua\sin\psi\,d\psi + \int_{a-\delta}^a v\,dr + \frac{1}{R+a\sin\psi}\frac{\partial}{\partial\theta}\int_{\psi}^{\frac{1}{2}\pi}\int_{a-\delta}^a awr\,dr\,d\psi = 0.$$

The first term of the above equation is the amount of fluid that enters or leaves the boundary layer between $\psi = 90°$ and any station $\psi$, the second term is the amount of fluid that flows through the boundary layer at the station $\psi$ and the third term is the change in flow rate in the boundary layer along the axial direction. Carrying out the above integrations with the help of (5), (6) and (10) gives

$$\delta_1\bar{v}_1 = \frac{1}{1+\alpha\sin\psi}\left\{-12f_3\cos\psi + 3(\pi - 2\psi + \sin 2\psi)\left(f_1' - \frac{f_2'}{1+\alpha\sin\psi}\right)\right.$$
$$\left. - 8\frac{\partial}{\partial\theta_1}\left[\bar{\delta}_1\left(f_1 + \frac{f_2}{1+\alpha\sin\psi}\right)(\tfrac{1}{2}\pi - \psi)\right]\right\}. \tag{15}$$

The thickness of the boundary layer can be determined from (11) with the help of (13) and (15):

$$\delta_1 = \Big[3{\cdot}75(\delta_1\bar{v}_1)\frac{\partial\delta_1\bar{v}_1}{\partial\psi}+\alpha\delta_1\bar{v}_1 - 2{\cdot}625\frac{(\delta_1\bar{v}_1)^2}{\bar{w}_0}\frac{\partial\bar{w}_0}{\partial\psi}+5{\cdot}25\frac{\bar{\delta}_1}{1+\alpha\sin\psi}\frac{\partial}{\partial\theta_1}(\delta_1\bar{v}_1\bar{w}_0) + \frac{7(\delta_1\bar{v}_1)}{1+\alpha\sin\psi}\left(\bar{w}_0\frac{d\bar{\delta}_1}{d\theta_1}+2\bar{\delta}_1\frac{\partial\bar{w}_0}{\partial\theta_1}\right)\Big]\Big/(-49\bar{w}_0^2\cos\psi). \tag{16}$$

## 5. Determinations of the functions $f_1$, $f_2$ and $f_3$

The momentum equations (11) and (12) for the boundary layer can be solved in terms of the outer solution for the inviscid flow through the unknown functions $f_1$, $f_2$ and $f_3$. These functions can be determined by matching the outer and inner solutions. Equation (15) shows that, for small $\alpha$, the mass flow rate $\delta\bar{v}_1$ has a maximum in the neighbourhood of $\psi = 0$ (and 180°). Physical intuition that the boundary layer acts as a reservoir, receiving fluid in the domain $180° \geqslant \psi \geqslant 0$ and losing it in the domain $0 \geqslant \psi \geqslant -180°$, suggests that the flow rate in the boundary layer will attain its maximum at $\psi = 0$ (and 180°). Since the variation of the boundary-layer thickness with respect to $\psi$ is small, the above argument can be replaced by the statement that $\bar{v}_1$ attains its maximum at $\psi = 0$ (and 180°), i.e.

$$\partial\bar{v}_1/\partial\psi = 0 \quad \text{at} \quad \psi = 0, 180°. \tag{17}$$

The axial velocity of the accelerating flow due to the displacement effect of the boundary layer is of order $1+O(\delta)$. From (6), it follows that $f_1 - f_2 = O(D^{-\frac{1}{2}})$, because $\delta$ is $O(D^{-\frac{1}{2}})$. From (15), we know that $f_1'$, $f_2'$ and $f_3$ are $O(D^{-\frac{1}{2}})$. Thus we conclude that $\theta_0$ will be $O(D^{\frac{1}{2}})$ when the flow approaches its fully developed state. With the above estimates, we can set†

$$\left.\begin{aligned} f_1(\theta_0) - f_2(\theta_0) &= 1 + g_1(\bar{\theta})\,D^{-\frac{1}{2}}, \\ f_2(\theta_0) = g_2(\bar{\theta})/\alpha, \quad f_3(\theta_0) &= g_3(\bar{\theta})\,D^{-\frac{1}{2}}, \end{aligned}\right\} \tag{18}$$

where $\bar{\theta} = \theta_0 D^{-\frac{1}{2}} = \theta_1 D^{-\frac{1}{2}}$ is the downstream variable characterizing the region where the flow is asymptotically approaching the fully developed state. Taking the derivative of (12) with respect to $\psi$ and rearranging (11) with the help of conditions (17) and (18), we obtain

$$\begin{aligned} \dot{g}_2 &= \{[36(g_2+2\alpha)^2 + 8(2-\alpha g_2+3(\alpha-1)g_2^2)]^{\frac{1}{2}} - 6(g_2+2\alpha)\}\,g_3/\pi \\ &= F(g_2;\alpha)\,g_3/\pi \end{aligned} \tag{19}$$

and

$$\dot{g}_2^3 + 3{\cdot}225\,g_2g_3\dot{g}_2^2 + 6{\cdot}45(g_2g_3)^2\dot{g}_2 + 4{\cdot}06(g_2g_3)^3 - 24{\cdot}1/g_3 + O(D^{-\frac{1}{2}}) = 0, \tag{20}$$

† It can be shown that equations (3), derived earlier using the previous scaling, are also valid in this region; i.e. equations (3) are uniformly valid at distances up to $O((aRD)^{\frac{1}{2}})$.

after neglecting smaller-order terms, where a dot over a function denotes its derivative with respect to $\bar{\theta}$. The required third relation between $f_1$, $f_2$ and $f_3$ is obtained from the assumption that the variation of the thickness of the boundary layer with respect to $\psi$ is small, i.e., $\bar{\delta}_1 = \delta_1|_{\psi=0}$. Combining this with (14), (16) and (18) yields

$$g_1 = \tfrac{2}{7}[15\pi \dot{g}_2 g_3 + 72 g_2 g_3^2]^{\frac{1}{2}}. \tag{21}$$

Equation (20) has lost its second-order derivative terms, indicating that this simplified form is not valid for small values of $\bar{\theta}$. It represents the downstream flow (in modern terminology, an outer solution). It does show that a much simpler relation exists among $g_1$, $g_2$ and $g_3$ away from the immediate neighbourhood of the entrance of the tube. Note particularly that the function $g_1$ is uncoupled from $g_2$ and $g_3$ in (19) and (20), and can be determined by (21) after the determination of $g_2$ and $g_3$ from (19) and (20). Eliminating $g_3$ between (19) and (20) gives

$$\dot{g}_2 = \left[\frac{24{\cdot}1}{F^3 + 3{\cdot}225\,F^2 g_2 + 6{\cdot}45\,F g_2^2 + 4{\cdot}06\,g_2^3}\right]^{\frac{1}{2}} F. \tag{22}$$

Substitution of (18) into (14) and (15) yields

$$\bar{\delta}_1 = 1{\cdot}5\,g_1(\bar{\theta})\,D^{-\frac{1}{2}}, \quad d\bar{\delta}_1/d\theta_1 = 1{\cdot}5\,\dot{g}_1(\bar{\theta})\,D^{-1}, \tag{23}$$

$$\delta_1 \bar{v}_1 = \frac{1}{1+\alpha\sin\psi}\left\{-12\,g_3\cos\psi + 3(\pi + 2\psi + \sin\psi)\left(\dot{g}_1 D^{-\frac{1}{2}} + \frac{\dot{g}_2\cos\psi}{1+\alpha\sin\psi}\right)\right.$$
$$\left. -\frac{8}{\alpha}\frac{d}{d\bar{\theta}}\left[1{\cdot}5\,g_1\left(\frac{\pi}{2}-\psi\right)(1 + g_2\sin\psi + O(\alpha)\right] D^{-\frac{1}{2}}\right\} D^{-\frac{1}{2}}. \tag{24}$$

Since the fully developed flow is independent of $\bar{\theta}$, the asymptotic values of $g_1$, $g_2$ and $g_3$ can be evaluated from (19)–(21) by setting the $\bar{\theta}$-derivative terms equal to zero, which gives

$$g_2 = \{[\alpha^2 + 24(1-\alpha)]^{\frac{1}{2}} - \alpha\}/6(1-\alpha),$$
$$g_3 = 1{\cdot}56/g_2^{\frac{3}{2}}, \quad g_1 = 2{\cdot}425 g_2^{\frac{1}{2}} g_3.$$

These relations agree with Barua's (1963) results for fully developed flow in a curved pipe.

For small $\bar{\theta}$, the first term of the series solution of (11) is equivalent to taking the limit of (11) as $\bar{\theta} \to 0$; doing so we obtain

$$\lim\left[\tfrac{1}{2}\partial(\delta_1 \bar{v}_1 \bar{w}_0)/\partial\bar{\theta} - \tfrac{7}{15}\delta_1 \bar{w}_0^2\right]_{\psi=0} = 0.$$

Rearrangement of the above relation and use of (18), (23) and (24) gives

$$\ddot{g}_2 = \tfrac{7}{6}\alpha(1 + g_1 D^{-\frac{1}{2}})\,D. \tag{25}$$

This is the upstream solution (or inner solution), which shows how the inviscid velocity profile adjusts itself to balance the centrifugal force when the fluid enters the curved pipe.

The initial conditions (4*a*), in terms of $g_1$, $g_2$ and $g_3$, are

$$g_1(0) = g_2(0) = g_3(0) = 0, \quad \dot{g}_1(0) = \dot{g}_2(0) = 0. \tag{26}$$

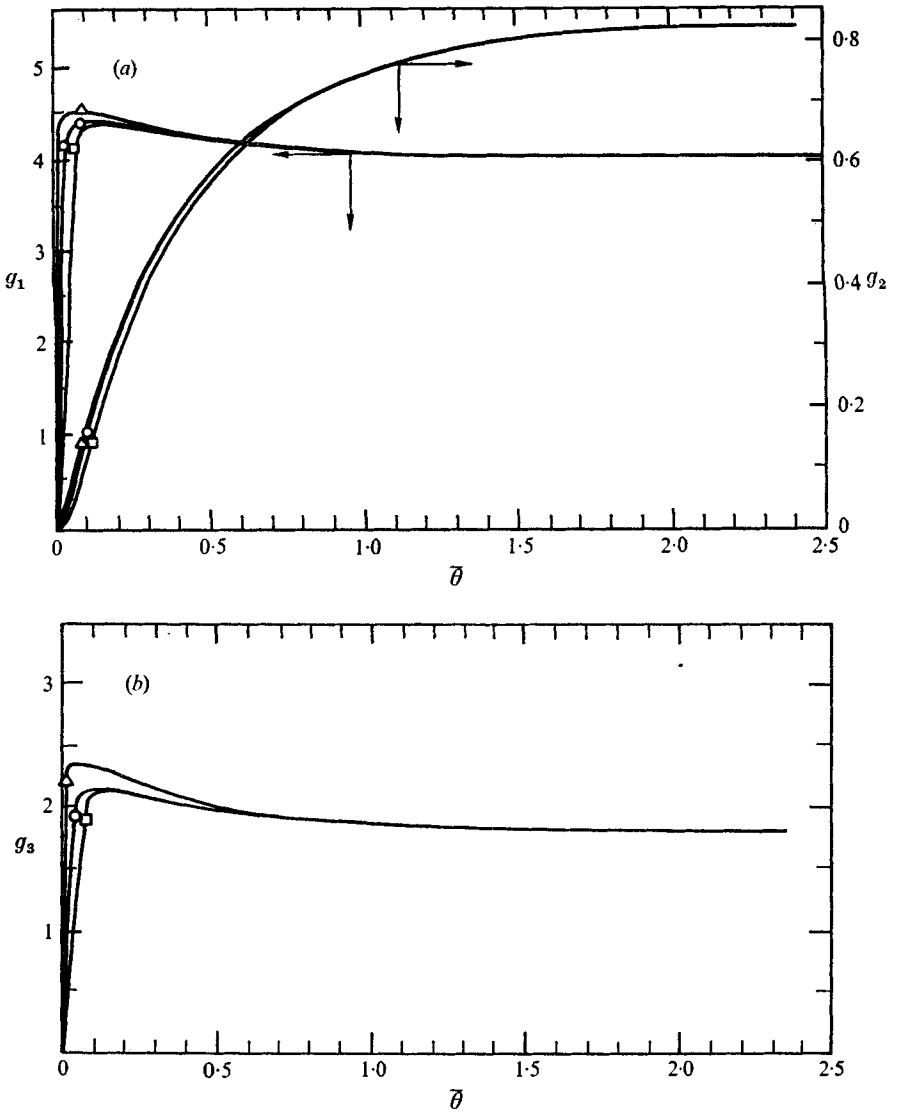


FIGURES 3(*a*, *b*). For legend see next page.

Thus, the values of $g_2$ can be determined as follows.

(i) Integrate (25) with conditions (26) for small $\bar{\theta}$.

(ii) Guess a value $\bar{\theta} = \bar{\theta}_m$ and evaluate $g_2(\bar{\theta}_m)$ and $\dot{g}_2(\bar{\theta}_m)$ from (25).

(iii) Evaluate $\dot{g}_2(\bar{\theta}_m) = \dot{g}_2[F(\bar{g}_2; \alpha)]$ from (22), where $\bar{g}_2 = g_2(\bar{\theta}_m)$.

(iv) Check that the difference between the values of $\dot{g}_2(\bar{\theta}_m)$ obtained from (25) and (22) respectively is less than $\epsilon$.

(v) Iterate the above four steps to get $\bar{\theta}_m$ and $g_2(\bar{\theta}_m)$ for $\epsilon \to 0$, which gives the continuous values of $g_2$ and $\dot{g}_2$ at $\bar{\theta} = \bar{\theta}_m$, i.e. a continuous velocity at $\bar{\theta} = \bar{\theta}_m$.

(vi) Use the Runge–Kutta scheme to integrate (22) numerically with the $g_2(\bar{\theta}_m)$ obtained in step (v).

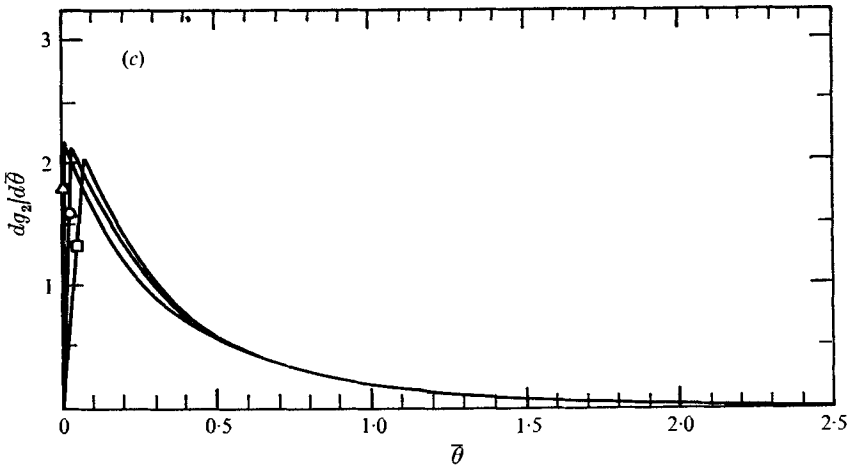


FIGURE 3. Functions (*a*) $g_1$ and $g_2$, (*b*) $g_3$ and (*c*) $dg_2/d\bar{\theta}$.

| | □ | ○ | △ |
|---|---|---|---|
| *Re* | 1000 | 2000 | 2000 |
| $\alpha$ | 0·05 | 0·05 | 0·1 |
| *D* | 447·21 | 894·43 | 1264·91 |

With $g_2$ known, $g_1$ and $g_3$ can easily be evaluated from (19) and (21).

The numerical results for $g_1$, $g_2$, $g_3$ and $\dot{g}_2$ are shown in figures 3(*a*)–(*c*) for different combinations of $\alpha$ and *Re*. The curves differ from each other in the domain close to the entrance, and asymptotically approach $\alpha$-dependent fully developed flow. Since the fully developed flow depends weakly on $\alpha$, the difference between the curves at this stage of the flow for different values of $\alpha$ is too small to be seen in these figures. Close to the entrance, the values of $g_1$, $g_2$, $g_3$ and $\dot{g}_2$ vary with Dean number. In figure 3 the steep initial rises in each of the functions plotted occur over a region whose extent is of order $(aR)^{\frac{1}{2}}$, the initial scale of $R\theta$.

## 6. Results and discussion

*Velocity distributions and secondary boundary-layer thickness*

The speed $\bar{v}_1$ of the secondary flow has been calculated from (13) for a Reynolds number of 2000 and $\alpha = 0{\cdot}05$, which corresponds to a Dean number of 894·43. The development of the secondary flow velocity along the pipe is shown in figure 4(*a*) for different $\psi$. The abrupt change in the curve for $\psi = -60°$ is due to separation of the boundary layer, which occurs in the neighbourhood of this angle, in agreement with Barua's analysis and Squire's measurements (Barua 1963). The location of the separation point as a function of distance down the pipe is presented in figure 4(*b*).

The distribution of the boundary-layer thickness for different $\psi$ as a function of $\bar{\theta}$ is plotted in figure 5. The occurrence of a maximum value for $\delta_1$ before the flow becomes fully developed indicates that the cross-flow in the central core of the tube prevents the boundary layer from diffusing further out. The curve

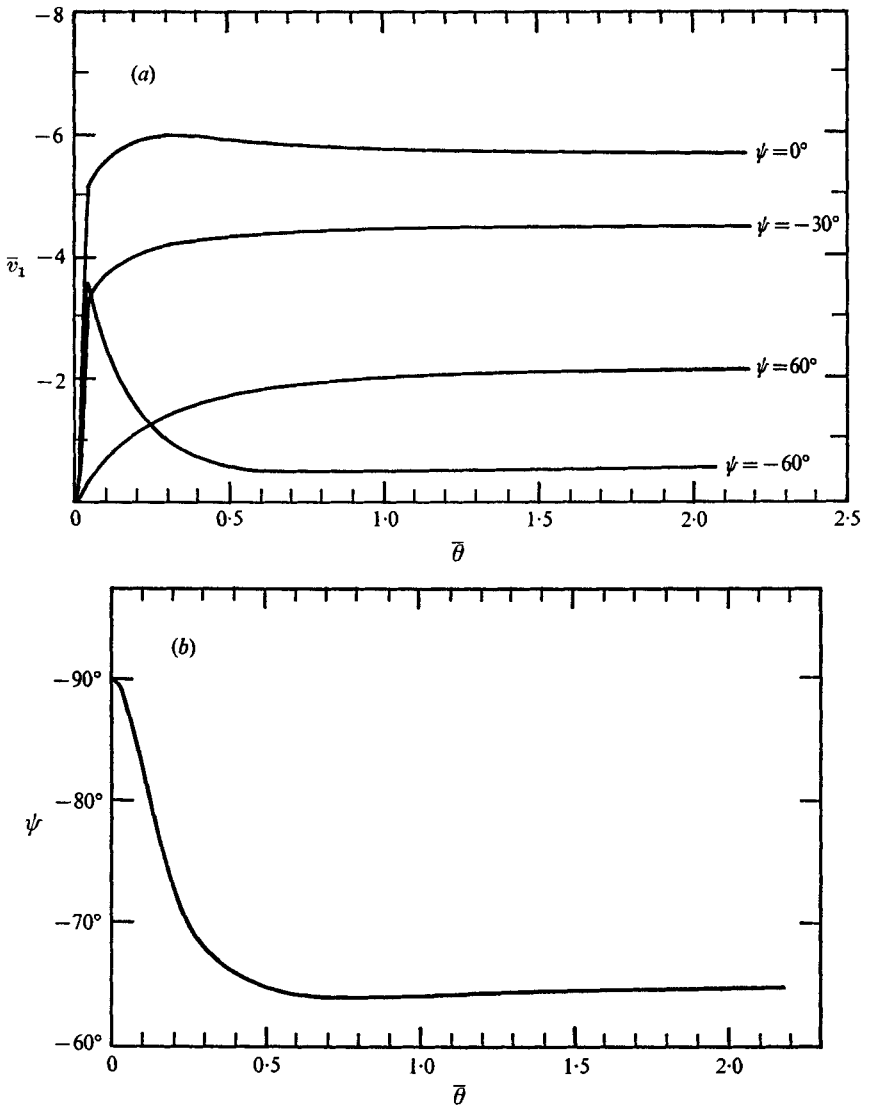


FIGURE 4. (*a*) Secondary flow velocity and (*b*) location of separation point as functions of downstream distance. $Re = 2000$, $\alpha = 0{\cdot}05$, $D = 894{\cdot}43$.

for $\psi = -60°$ in figure 5 shows that the boundary layer grows very rapidly near the separation point. The distributions of the velocity $\bar{v}_1$ and the boundary-layer thickness $\delta_1$ over each cross-section are shown in figures 6(*a*) and (*b*).

### *Pressure drop*

The fluid flow along the pipe is accompanied by a fall in the pressure head. The pressure gradient along the pipe can be evaluated from (5*c*):

$$\frac{1}{R}\frac{\partial P}{\partial \theta} = -\frac{\rho \bar{W}^2}{(aR)^{\frac{1}{2}}}(1+\alpha r_0)\left[u_0\frac{\partial w_0}{\partial r_0}+\frac{w_0}{1+\alpha r_0}\frac{\partial w_0}{\partial \theta_0}+\frac{\alpha u_0 w_0}{1+\alpha r_0}\right].$$

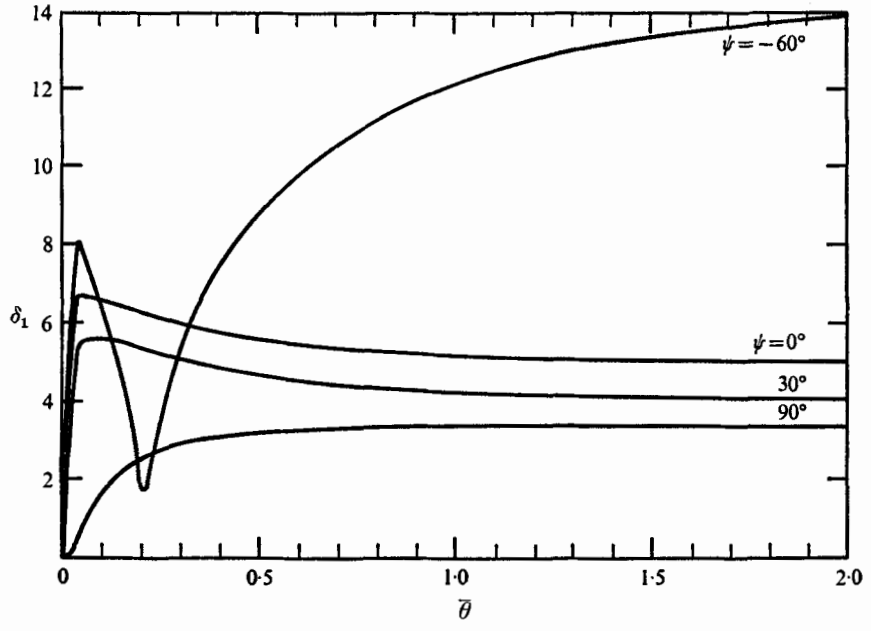


FIGURE 5. Boundary-layer thickness. $Re = 2000$, $\alpha = 0{\cdot}05$, $D = 894{\cdot}43$.

Rewriting this in terms of the functions $f_1, f_2$ and $f_3$ gives

$$\frac{1}{R}\frac{\partial P}{\partial \theta} = -\frac{\rho W^2}{(aR)^{\frac{1}{2}}}\left[\frac{\alpha f_1 f_3}{1+\alpha r_0} + \frac{\alpha r_0 f_1}{1+\alpha r_0}\left(\frac{f_2'}{1+\alpha r_0} - f_1'\right) + \left(f_1 - \frac{f_2}{1+\alpha r_0}\right)\left(f_1' - \frac{f_2'}{1+\alpha r_0}\right)\right]. \tag{27}$$

The first term on the right-hand side is the pressure gradient needed to maintain the flow pattern under the centrifugal force. The other terms represent the pressure gradient which is necessary to accelerate the fluid flowing along the pipe owing to the displacement effect of the boundary layer and interaction between cross-flow and accelerating flow. From relations (18) we can see that the pressure gradient due to viscous effects is of smaller order than that due to the inertia effect, represented by the first term. This is so because the boundary layer is very thin and the acceleration of the main flow due to the displacement effect is small.

Substitution of (18) into (27) allows us to write

$$\frac{1}{R}\frac{\partial P}{\partial \theta} = -\frac{\rho \overline{W}^2}{(aR)^{\frac{1}{2}}}\left[\frac{(\alpha+g_2)\,g_3}{1+\alpha r_0} + \frac{r_0 \dot{g}_2}{(1+\alpha r_0)^2}\right] D^{-\frac{1}{2}} + O(D^{-1}).$$

To evaluate the pressure drop along the pipe, the mean value of the pressure gradient over the cross-section is introduced:

$$\overline{\frac{1}{R}\frac{\partial P}{\partial \theta}} = \frac{1}{A}\int_A \frac{1}{R}\frac{\partial P}{\partial \theta}\,dA,$$

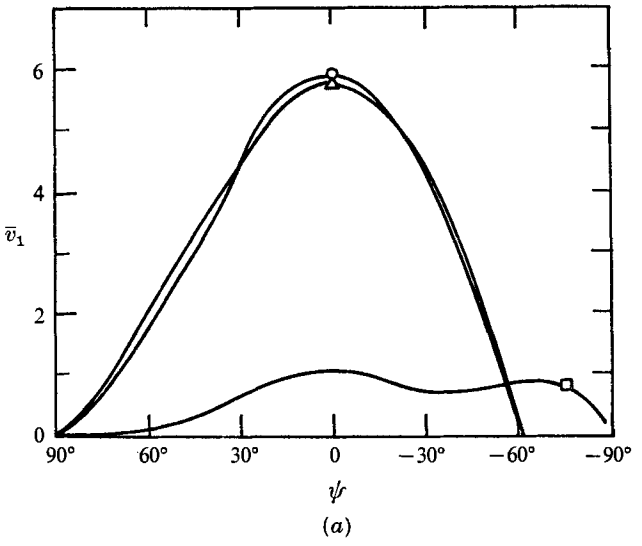


(*a*)

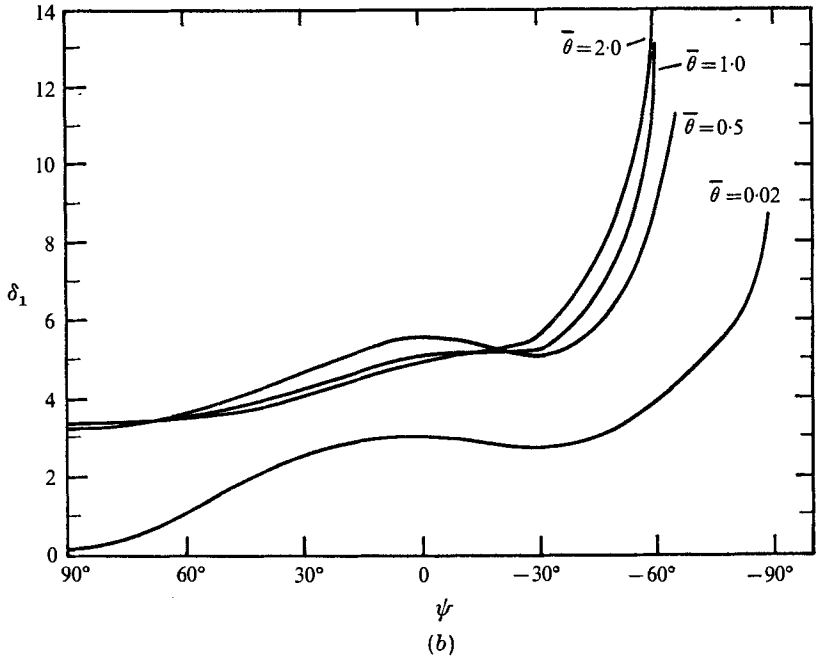


(*b*)

FIGURE 6. Distribution of (*a*) secondary flow velocity and (*b*) boundary-layer thickness over each cross-section. $Re = 2000$, $\alpha = 0{\cdot}05$, $D = 894{\cdot}43$. (*a*) □, $\bar{\theta} = 0{\cdot}02$; ○, $\bar{\theta} = 0{\cdot}5$; △, $\bar{\theta} = 1{\cdot}0$.

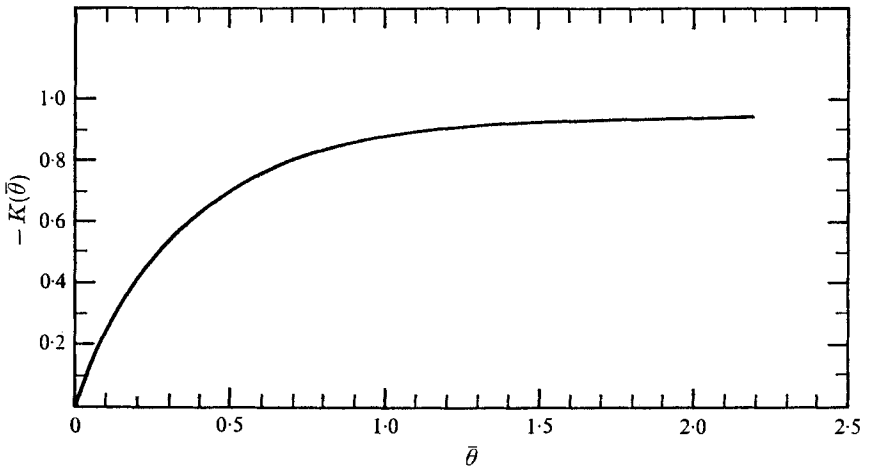


FIGURE 7. The function $K(\bar{\theta})$. $Re = 2000$, $\alpha = 0{\cdot}05$, $D = 894{\cdot}43$.

where $A = \pi a^2$ is the cross-sectional area of the pipe. Thus,

$$\frac{\overline{1}}{R}\frac{\overline{\partial P}}{\partial\theta} = -\frac{\rho\overline{W}^2}{(aR)^{\frac{1}{2}}}\left[\frac{(\alpha+g_2)\,g_3}{1-\alpha^2}\right]D^{-\frac{1}{2}}+O(D^{-1}).$$

Integration of this equation along the axis of the pipe, starting at the entrance, gives

$$\frac{P^0-P}{\frac{1}{2}\rho\overline{W}^2} = 2\int_0^{\bar{\theta}}\left[\frac{(\alpha+g_2)\,g_3}{1-\alpha^2}\right]d\bar{\theta}, \tag{28}$$

where $P^0$ is the pressure at the entrance. Defining the pressure difference $K(\bar{\theta})$ between the developing flow and the fully developed flow as

$$K(\bar{\theta}) = 2\int_0^{\bar{\theta}}\left[\frac{(\alpha+g_2)\,g_3}{1-\alpha^2}\right]d\bar{\theta}-\frac{2}{1-\alpha^2}[\alpha+g_2(\infty)]\,g_3(\infty)\,\bar{\theta},$$

(28) becomes

$$\frac{P^0-P}{\frac{1}{2}\rho\overline{W}^2} = K(\bar{\theta})+(\Delta P)_f, \tag{29}$$

where $(\Delta P)_f = 2[\alpha+g_2(\infty)]\,g_3(\infty)\,\bar{\theta}/(1-\alpha)^2$ is the pressure drop for the fully developed flow. The values of $K(\bar{\theta})$ for $Re = 2000$ and $\alpha = 0{\cdot}05$ are presented in figure 7, which shows that the pressure drop in the entry region is in fact less than the loss of pressure head necessary to maintain the fully developed flow. This perhaps surprising result is a consequence of the fact that the cross-flow in the entrance region is smaller than that for the fully developed flow.

### *The length of the entry region*

The length of the entry region can be defined as that value of $\bar{\theta}$ at which the function $g_2$ takes on 99 % of its value for the fully developed flow. The length of the entry flow is conveniently written as

$$l_c = e_1(D/\alpha)^{\frac{1}{2}}a. \tag{30}$$

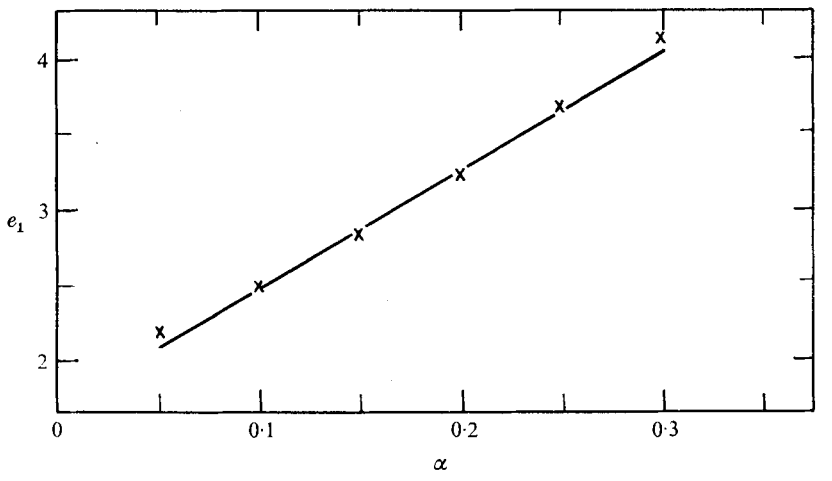


FIGURE 8. Coefficient of entry length.

The values of $e_1$ turn out to be weakly dependent on the values of $\alpha$, and are not sensitive to the Reynolds number. Typical values of $e_1$, as plotted in figure 8, can be represented by a straight line within the range of practical interest.

The entry length for straight tubes is approximately (Fargie & Martin 1971)

$$l_s = 0{\cdot}25\, a\, Re. \tag{31}$$

The ratio of (30) to (31) is

$$l_c/l_s = 8e_1/D^{\frac{1}{2}}, \tag{32}$$

which shows that the entry length for a curved pipe, for large $D$, is much shorter than that for the corresponding straight tube. For $\alpha = 0{\cdot}05$ and $Re = 2000$, for which $D = 894{\cdot}43$, we find that $l_c/l_s = 0{\cdot}584$. For this typical value, the entry length is approximately equal to half that for a straight pipe.

In view of the various approximations involved, perhaps no more than a qualitative validity can be claimed for these results. The assumption that outside the boundary layer the motion is confined to planes parallel to the plane of symmetry of the tube is perhaps drastic and is not strictly valid in the region near the entrance and the pipe wall; its validity, however, should improve as the flow approaches the fully developed state. Furthermore, the assumed simple expression for the inviscid velocity is in the nature of a perturbation of the fully developed flow. In spite of the simplifications adopted in the analysis, this model, at least, fulfils the purpose of describing clearly the characteristics and behaviour of the entry flow in curved pipes. This effort can give guidance to future numerical work on the same subject. Also, the analysis exposes the analytical dependence of the problem, which is implicitly involved in the analysis and would be impossible to detect without going through a similar procedure. Certainly knowing correct scales is important in treating experimental data. Ultimately, the accuracy of the analysis would have to be verified by numerical integration of the Navier–Stokes equations, or from reliable experimental data.

This work was supported by the National Science Foundation under Grant ENG 73–03970 A 01.

## REFERENCES

BARUA, S. N. 1963 *Quart. J. Mech. Appl. Math.* **16**, 61.

BRILEY, W. R. 1972 *Proc. 3rd Int. Conf. Numerical Methods in Fluid Dynamics, Paris* 1972, pp. 33–38.

DEAN, W. R. 1927 *Phil. Mag.* **4**, 208.

DEAN, W. R. 1928 *Phil. Mag.* **5**, 673.

EUSTICE, J. 1911 *Proc. Roy. Soc.* A **85**, 119.

FARGIE, D. & MARTIN, B. W. 1971 *Proc. Roy. Soc.* A **321**, 461.

GREENSPAN, D. 1973 *J. Fluid Mech.* **57**, 167.

KUCHAR, N. R. & OSTRACH, S. 1971 *A.I.A.A. J.* **9**, 1520.

LYNE, W. 1970 *J. Fluid Mech.* **45**, 13.

MCCONALOGUE, D. J. & SRIVASTAVA, R. S. 1968 *Proc. Roy. Soc.* A **307**, 37.

MORIHARA, H. & CHENG, T. S. 1973 *J. Comp. Phys.* **11**, 550.

SINGH, M. P. 1974 *J. Fluid Mech.* **65**, 517.

TAYLOR, G. I. 1929 *Proc. Roy. Soc.* A **124**, 243.

VAN DYKE, M. D. 1970 *J. Fluid Mech.* **44**, 813.

WILSON, S. D. R. 1971 *J. Fluid Mech.* **46**, 787.

YAO, L. S. 1973 Ph.D. thesis, Department of Mechanical Engineering, University of California, Berkeley.

ZALOSH, R. G. & NELSON, W. G. 1973 *J. Fluid Mech.* **59**, 693.